An analysis methodology for long vertical line-shaft pumps with hydrodynamic bearings

D White, T Bracey
DC White Consulting Engineers Limited, United Kingdom

Abstract

The long drive shafts of vertical axis line-shaft pumps are usually guided by water-lubricated self-acting journal bearings. When aligned vertically these bearings have no static load, so no linearised radial stiffness. Industry codes often stipulate linear lateral critical speed criteria, and appear not to appreciate the dominance of non-linearity, as reflected in the academic literature. This paper presents a new methodology and underlying bespoke software, which shifts the criteria towards predicting bearing loads, housing vibrations and modal mass rather than just critical speeds. Following review, this approach has been accepted by various companies and institutions for dozens of pumps.

1. INTRODUCTION

This paper describes an approach to assess the lateral vibration characteristics of a vertical shaft system lubricated by self-acting water bearings, typically employed for pumping sea water fire-fighting systems. Pumps are typically made up of 20m to 50m long train of connected drive shaft sections with impellors at the bottom, concentric within a train of stationary columns which support the drive via bearings at each flange, typically at 2m to 3m centres.

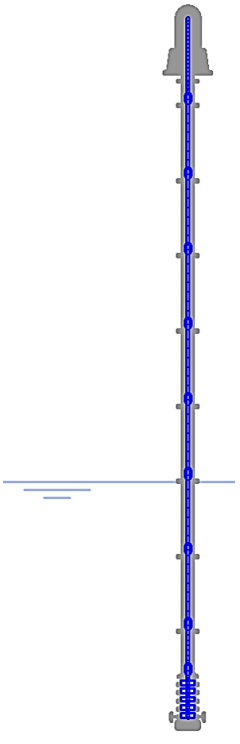

Left: Figure 1 – Typical pump layout and water level

Lateral vibration analyses as per API 610 (1) fall into two categories: 'rigid' (or rather, 'classically stiff') and 'flexible'. Rigid rotor systems run below their fundamental lateral critical speeds when analysed as having infinitely stiff bearings. The classification of 'flexible' otherwise applies, requiring dynamic analyses incorporating the finite stiffness and clearances of the bearings. The bearings are often axially fluted rubber water-lubricated journal bearings, concentric with the shaft sleeves, typically 70mm to 120mm in diameter at the rotor-stator interface. These have proved highly effective in practice, but their use with vertical axis concentric shafting has received little attention in the academic literature, despite substantial attention to horizontal axis devices.

When aligned vertically these bearings have no static load and hence no linearised radial stiffness. Thus the use of lateral critical speeds, a linear phenomenon, to infer vibration levels in a rotor dominated by non-linearity is a non-sequitur. Industry codes such as NFPA 20 (6) stipulate critical speed separation margins of ±25% from the running speed, and we find that any realistic bearing treatment (as herein discussed) will fail this test, calling designs with half a century of pedigree needlessly into question.

Further, classification as a 'rigid' rotor system is often technically possible for bearing spans of up to 2 metres when assuming infinite bearing stiffness. In these cases, the damped imbalance response tends to produce vibration amplitudes well below the bearing clearances, making the assumption of infinite bearing stiffness absurd. This is a game of semantics best avoided; a thorough understanding is needed.

2. BEARING MODEL OVERVIEW

Within these water-lubricated bearings, hydrodynamic positive pressures are created by drawing water into a converging clearance and negative pressures in a diverging clearance.

The pressure field can be determined analytically using the widely applied Euler film equation, which is a simplification of the Navier-Stokes equations. The variation of bearing radial and tangential hydrodynamic forces versus the eccentricity ε (the relative offset of the axes between the rotor and housing, non-dimensionalised by the radial clearance) can be computed. This gives the bearing constants, feeding into an analysis of the entire rotor system. This treatment is well established, and bearing manufacturers often have proprietary software to turn bearing geometries into dynamic characteristics, often with high sophistication.

Normally, a static load would bias a horizontal shaft into an eccentric equilibrium position, and small vibrations would trace out elliptical orbits, giving linearised stiffness and damping coefficients about that point. However for a concentric orbit, reference (2) equation (6-16) gives the dynamic radial force (in the rotating frame) for an 'uncavitated long bearing' as:

$$F_r = -12\mu RL\left(\frac{R}{C}\right)^2 \frac{\pi\dot{\varepsilon}}{(1-\varepsilon^2)^{\frac{3}{2}}}$$

(A 'long' bearing disregards the end effects, so has a closed-form solution, but the principle stands.) With no static load, and hence a circular concentric orbit, the dimensionless radial velocity $\dot{\varepsilon}$ is zero at any eccentricity ε, so the radial stiffness must also be zero. (This assumes no cavitation, as discussed below.)

The point is subtle, but upon realisation one might wonder why these bearings are used in the vertical axis at all if they offer no stiffness. Rubber self-lubricated journals are very good value, have decent dry lubrication properties and they tolerate impact and sliding for the short duration of dry start-up. The prediction of any actual hydrodynamic effect has not been the driving force behind their evolution. These bearings typically have 8 to 10 axial grooves to improve the admission of lubricating water and the expulsion of contaminants. These will keep the film pressures at the edges of the lands at the local water pressure, greatly reducing the magnitude of the pressures developed. Figure 2 shows a typical unwrapped pressure map for the Euler film equation, computed using an in-house solver.

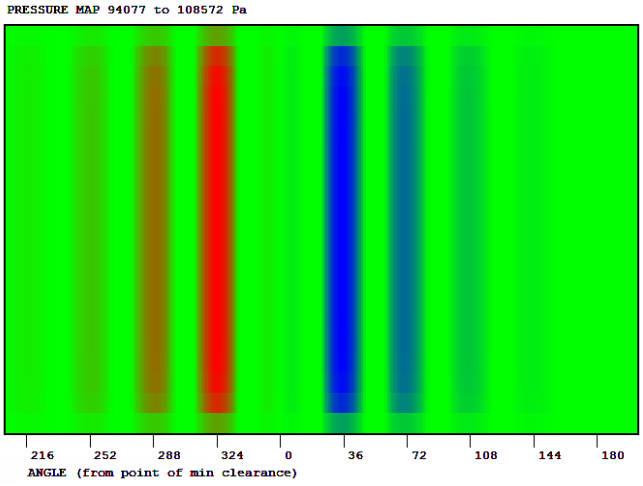

Figure 2- Typical Bearing Pressure Map for Parallel Eccentricity of 0.5.

This field produces non-zero damping, as per a classic uncavitated bearing.

The bearing film in figure 2 is 160 mm long (i.e. along the pump axis), 80 mm in diameter, has 10 lands, each 17.5 mm wide, and a concentric radial clearance of 91 µm. Sea-water properties are assumed at 10°C. At an eccentricity of 0.5 this produces peak land pressures of ±7,427Pag (±1.05 psig) at 1,750 rpm, creating a linearised damping of 4,000 N.s/m. At eccentricities of 0.25 and 0.75, the damping is computed at 2,770 N.s/m and 8,520 N.s/m respectively.

The load-carrying characteristics of the bearing are determined not only by the hydrodynamics but also how the rubber deflects under pressure, changing the size of the film under load. This problem was addressed by coupling the numerical solution of the Euler film equation to a finite element model of the rubber surface of one bearing groove. The stiffness of this groove was defined at discrete points, and a unit displacement was applied to each node whilst constraining the remainder. The reaction forces seen at each node represent a row of the inverted stiffness matrix.

Cabrera et al (3) makes the salient point that the high Poisson's ratio of rubber means that any inward deflection under high pressure at one location requires an almost equal volume of outward deflection elsewhere. Cabrera observed that static loading on a rubber bearing thus created pinch-points in the fluid film towards the outer edges of the lands, creating pressure spikes with a plateau in between. The effect of the Euler film equation appeared to be present but was far from dominant.

It was found that with a concentric orbit having an eccentricity of 0.75 of the clearance, the hydrodynamic pressures caused rubber deformations of only several microns. Thus the behaviour would effectively be the same as a rigid journal. Even at higher eccentricities, our results could not reproduce Cabrera's phenomenon for an axially grooved bearing, most likely because the many grooves offer the rubber space to expand circumferentially rather than radially. (When the pinch-points were artificially introduced, the general shape of the pressure profile seen by Cabrera was however reproduced.)

One crucial difference between grooved and un-grooved bearings is that short lands typically develop only small gauge pressures. Vance (2) describes how the suctions

created by a diverging cavity are often disregarded below around -5 psig (-34,474 Pag), even though well above the fluid's saturation vapour pressure. This could be more due to dissolved oxygen being pulled from solution than cavitation per se. The effect of disregarding the negative gauge pressure (often termed a 'pi-film' since only half of the bearing with the positive pressure is treated as active) is to create a net force with a component of stiffness. However, with short lands the suctions predicted by the Euler film equation are very modest (in the above case 7247 Pa, -1.05 psig), and so this 'cavitation' effect would on this basis not be expected. Thus the pressure field would be a 'two-pi-film' so would not create a component of stiffness for a concentric orbit, but does create a damping term.

This of course has to break down when the shaft meets the bearing under high excitation, and several additional physical mechanisms are invoked within a small span of eccentricity:

- The lubrication will cease and the Euler film equation must break down.
- The effect of rubber deflection may or may not create constrictions, depending on the groove geometry.
- The bearing stiffness (as viewed by the rotor) will asymptote towards being stiffly coupled to the stator as rubber-to-metal contact is established.
- The rubber will apply some friction force at any contact points, subject to some level of lubrication.

All of these effects are coupled, and the problem quickly becomes very complicated. However, the bearing force would increase rapidly, transitioning from relatively flexible to relatively stiff compared with the shaft flexure terms within a very narrow window of eccentricity. The bearing stiffness would thus abruptly adopt the static stiffness of the rubber (as part of the column stator train). It is deemed sufficient to apply zero radial stiffness for low eccentricities, and a very high radial stiffness when rubber-to-metal contact is established. In developing the procedures described here, it was found that applying a high secant radial stiffness was very unstable for multi-degree of freedom systems. Instead, an contact logic routine was set up to solve sequentially for all the contact forces required to constrain the rotor to within any bearing displaying contact, and using an assumed friction coefficient.

Since the damping does not substantially affect the critical speeds, it can be linearised at a value determined by iteration.

3. SOLVER DESCRIPTION

The complex behaviour of the pump system was analysed using an in-house finite element beam solver. This has been verified using several back-to-back comparisons with full three-dimensional finite element models assuming linearised bearing stiffness. In broad outline, the solver constructs two-noded vertical beam elements, each node with a complex lateral and rotational degree of freedom. The Euler-Bernoulli beam formulation written as part of a damped system takes the following form:

$$\begin{pmatrix} f_{1y} \\ m_1 \\ f_{2y} \\ m_2 \end{pmatrix} = \left[\frac{EI}{L^3} \cdot \begin{pmatrix} 12 & 6L & -12 & 6L \\ 6L & 4L^2 & -6L & 2L^2 \\ -12 & -6L & 12 & -6L \\ 6L & 2L^2 & -6L & 4L^2 \end{pmatrix} + i\omega C - \omega^2 \cdot \begin{pmatrix} M_1 & 0 & 0 & 0 \\ 0 & J_{t1} & 0 & 0 \\ 0 & 0 & M_2 & 0 \\ 0 & 0 & 0 & J_{t2} \end{pmatrix} \right] \cdot \begin{pmatrix} d_1 \\ \varphi_1 \\ d_2 \\ \varphi_2 \end{pmatrix}$$

The excitation forces and moments are on the left hand side, and internal forces are on the right including flexural stiffness, damping and inertia.

Gyroscopic effects are also modelled using the formulation of Genta (4), creating skew-symmetric transverse rotational inertia terms. (Given the slenderness of the system, the effect is small.) Gravity and thrust are also included as stiffening effects; pump thrust being simplified as varying with the speed squared. Both the mass of internal water and external virtual water mass were included.

At increments of 1 rpm, the solver assembles a complex dynamic structural stiffness matrix by superimposing adjacent element equations. Since the damping model is conceived on the basis of known dashpot constants (rather than using a modal or Rayleigh damping model) and, given that gyroscopic effects are included, the full dynamic coupling matrix has to be inverted at each speed. Given the modest number of degrees of freedoms (typically around 500 to 1000), this is numerically undemanding. Columns of the inverse matrix can be populated via a sparse BiCGSTAB method by setting the respective source terms to unity.

The force excitation vector (defined in the real plane) is derived by assuming each element carries the given balance-grade of G2.5, using the method as defined in reference (5). This gives a force per unit mass which is applied to each rotor element. A typical pump at 1800 rpm will have a total excitation force of around 500N distributed along its length, perhaps 30N of which for each impeller. The sign of this load over the rotor elements is highly influential, so the mode shapes nearest to the running speed are computed and then the signs of the excitation forces are matched in sympathy. Figure 3 shows a typical response curve, biasing the excitation to two modes near the running speed.

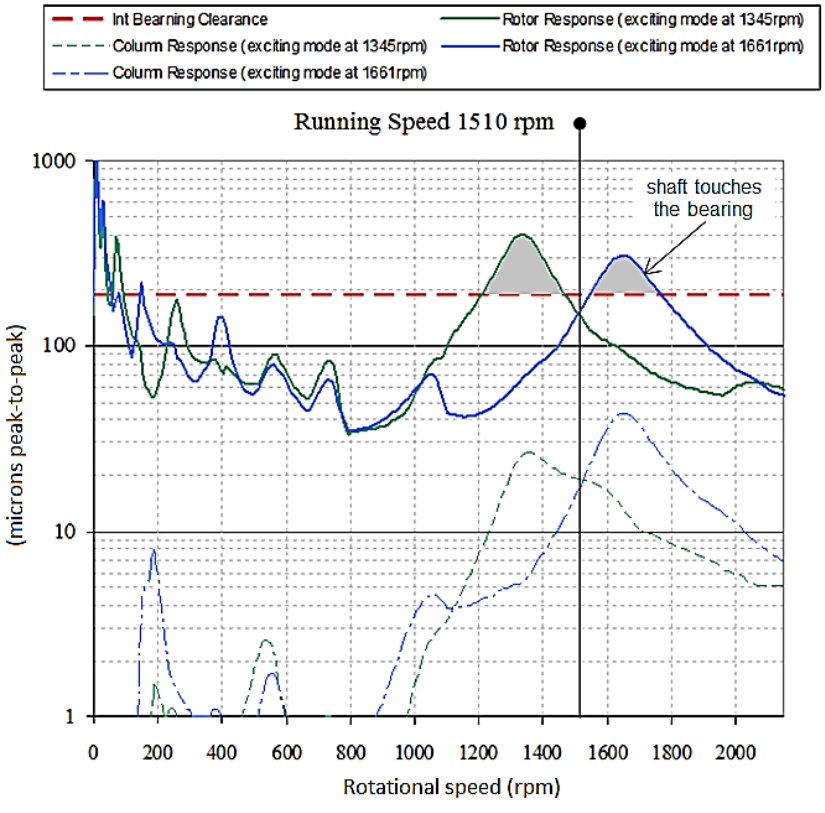

Figure 3- Typical system response vs running speed without contact

This indicates that the shaft will touch the journals at certain speeds when not using the contact model. Contact is handled within the software as an additional constraining force. The magnitude and direction is computed after the no-contact scenario and superimposed.

First we define the required displacement in a rotating Argand plane, defined as real in the plane of the signed excitation vectors. Applying a force in a given direction will at equilibrium cause the displacement to move in a direction rotating in the anti-clockwise sense by a compliance angle $\kappa = \tan^{-1} [\ Im(\mathbf{S^{-1}}_{i,i}) / Re(\mathbf{S^{-1}}_{i,i})\ ]$ where $\mathbf{S^{-1}}$ is the inverted dynamic stiffness matrix (the compliance matrix), and (i,i) the diagonal indices. This is depicted in the left of Figure 4.

Since the contact force is applied at the final location, the friction angle μ must be applied at this hitherto unknown position. The problem is solved trigonometrically, as shown in the right of Figure 4.

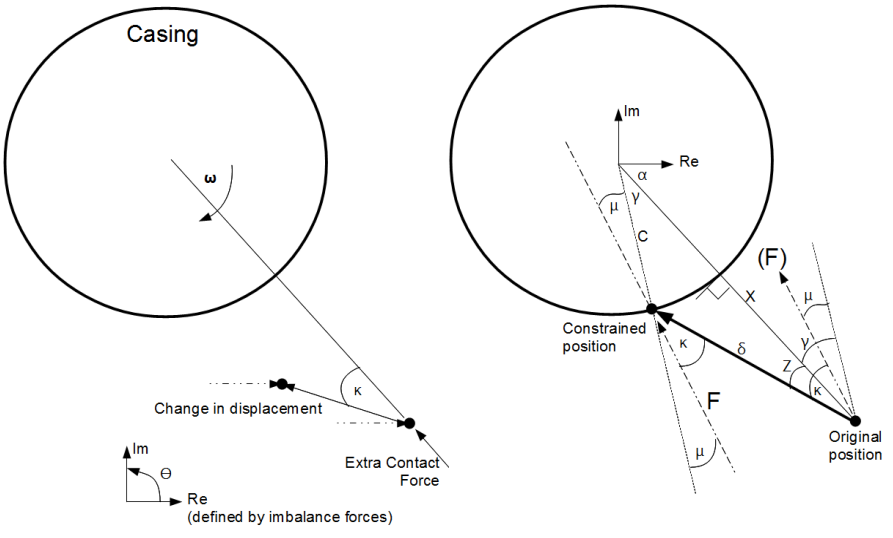

Figure 4 - (left) Depiction of compliance angle,
(right) Definition of constrained position

With X being the complex initial position (prior to applying contact model), C the bearing clearance, and α and γ defined as depicted, the desired displacement vector δ can be shown to satisfy:

$$Re(\delta) = - Re(X) + C \cos(\gamma + \alpha)$$
$$Im(\delta) = - Im(X) - C \sin(\gamma + \alpha)$$

The required complex constraining force f_i is then computed from the complex compliance matrix $\mathbf{S^{-1}}$ to satisfy the complex displacement δ.

When more than one bearing is predicted to be in contact (generally the case), the different contact forces need to be solved simultaneously. The procedure is to first solve without contact, then find the 'worst offending' node, apply the required constraining force, re-compute all displacements to find the new 'worst offending' node, and so on. Then a small matrix is set up to solve this along with the existing contacts, and this is repeated until all the bearings satisfy the contact constraints.

In each case, an equal and opposite force is applied to the vertical column tube, and the weak coupling is iterated to convergence.

Figure 5 shows a frequency response with these constraining forces included.

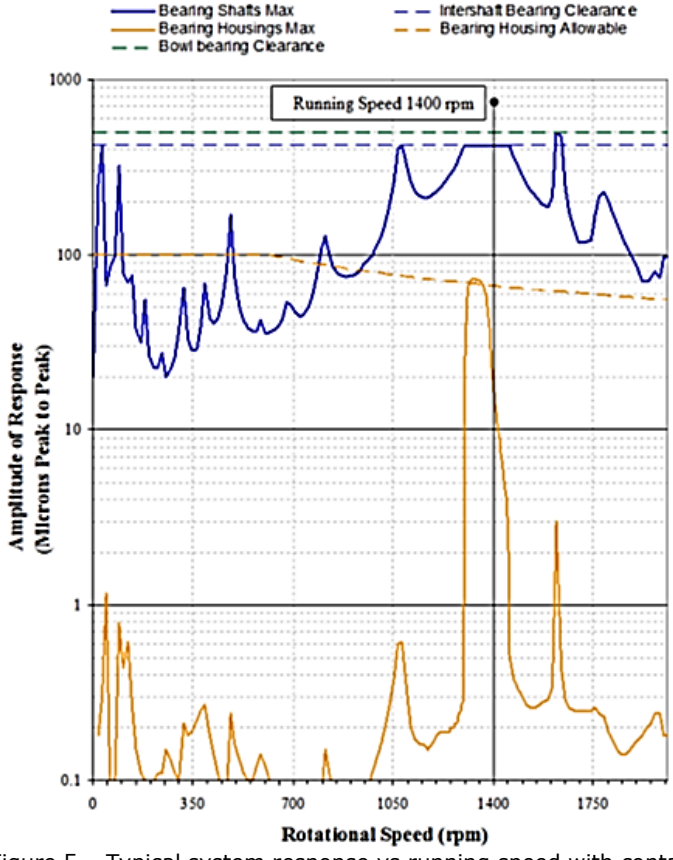

Figure 5 – Typical system response vs running speed with contact

4. PROPOSED ANALYSIS CRITERIA

The bearing damping forces are usually in the order of 1N to 10N, and any constraining forces can increase this up to around 500N. The manufacturer's practical design loading for bearing life at continuous running gives capacities typically around 2kN to 5kN, showing a fair margin. These bearings are found to wear in the field, so the activity of quantifying the loading provides a metric to compare new pump designs to existing pumps in the field, thereby providing reassurance that wear will not be unduly accelerated by any dynamic behaviour.

The stator displacements can also be quantified and compared to criteria such as API 610. Rotor modal mass participations are a further metric, but these are believed to be less instructive.

Different designs of pump will vary key parameters such as the overall length, the span of each column and rotor section, shaft diameters, bearing clearances, speed and design duty thrust. No matter the system however, the linear critical speeds

will populate a list of 20 or more modes. With critical speeds near the running speed having a separation of typically 10% to 20%, the separation margins are often far smaller, sometimes 0%, rarely achieving the target ±25%. The potential errors in the dynamics and hence critical speeds are comparable to separation margins in at least some cases. For this reason, the method considers bearing loads and column vibrations as if running the pump directly at the nearest pair of critical speeds, rather than just the running speed. This goes most of the way to mitigating errors in the dynamics.

Studies for bearings with new (unworn) and double clearances are also routinely run. The characteristic damping is typically about 4-5% of critical damping for unworn clearances, falling to around 0.5% when worn to double clearances. Two effects here compete: 1) the reduced damping increases rotor resonant response, and 2) larger clearances tend to prevent contact, reducing the vibration transmitted to the columns and hence cross-talk.

Variations of water level (and hence where column virtual water mass is applied) are also considered, although the effect on the column modes has little impact on rotor, although can encourage rotor-stator cross-talk, as was the case in Figure 5.

Problematic bearing loads and column vibrations are rarely predicted, as indeed is observed in reality. In the rare case illustrated in Figure 5, the column marginally exceeded the API 610 criteria for a narrow speed range, although this was discretionarily accepted. Compared to rotating systems in general, the acceptability of these pumps is actually quite insensitive to the main design parameters, as even the resonant response tends to prove acceptable. It is believed that practical issues such as the concentricity of the shafting relative to the column, the gearbox condition, the stiffness of the foundations, and the size and quantity of water impurities are bigger factors than the dynamics in determining a line-shaft pump's vibration levels.

5. CONCLUDING REMARKS

Together, these new metrics provide a better means of substantiation than existing industry codes.

This method bears the burden of self-justification, and yet has succeeded in many levels of proprietary review. However, a universally accredited method would be better for all parties.

A further burden is that full-scale instrumented testing of a, say, 50m long marine device is difficult to economically justify, given the half-century pedigree of successful use. Although it would miss the important point about the imbalance signs along the rotor, testing on individual vertical axis bearings would be a sensible starting point. It appears that manufacturers (on whom this duty would normally fall) are no more aware of the analytical issues herein described than the industry codes or academic literature. Instrumented empirical validation is required to elevate the authority of this method, and this publication hopes to raise consciousness.

The lack of detail in industry codes and the academic literature on vertical axis journal bearings might actually reflect their enduring success in the field. However, modern practice is heading toward analysis over 'appeal to prior experience', and it is inevitable that some older problems require renewed attention.

6. REFERENCES

1. API 610 Centrifugal Pumps for Petroleum, Petrochemical and Natural Gas Industries, Eleventh Edition, July 2011
2. J M Vance, "Rotordynamics of Turbomachinery", Wiley 1988
3. D L Cabrera et al, "Film pressure distribution in water-lubricated rubber journal bearings" IMechE 2005
4. G Genta, "Dynamics of Rotating Systems", Springer 2005
5. Mechanical vibration - Balance quality requirements for rotors in a constant (rigid) state, ISO 1940-1:2003
6. NFPA 20: Standard for the Installation of Stationary Pumps for Fire Protection, 2016 Edition